Difference of LAGEOS satellite response from raw data analysis of the collocation experiment between the Grasse Satellite and Lunar Laser Ranging stations

Joëlle NICOLAS, Jean-François MANGIN, Gilles MÉTRIS, and François BARLIER

Observatoire de la Côte d'Azur - CERGA
Avenue N. Copernic - F-06130 Grasse – France
Contact : Joelle.Nicolas@obs-azur.fr – Tel.: 00-33-493.405.381 – Fax.: 00-33.493.405.333

Abstract

We performed a collocation experiment at the Grasse observatory (France) between three independent laser ranging instruments: the Satellite Laser Ranging (SLR), the Lunar Laser Ranging (LLR) station, and the French Transportable Laser Ranging Station (FTLRS). The normal point analysis of the common passes on LAGEOS –1 and –2 satellites showed a systematic difference of 13 mm between the SLR and the LLR station results. 9 mm are already explained with instrumental reasons for the LLR station (photodiode center-edge effect and velocity aberration). To explain the residual bias, from raw data and geometrical analysis, we computed the difference of the LAGEOS satellite ranges due to instrumental differences. We show that the satellite signature effectively depends on the station at the level of 3 mm. Thus, we are able to explain at the 1 mm level the bias difference of 12 mm between the 2 considered stations. We also propose to adopt a LAGEOS center of mass correction value depending on the laser ranging station technical features, dependency especially coming from the difference between single and multi photoelectron detection levels. We found that this difference can reach a few millimeters with resect to the standard value used for the laser ranging data analysis.

1. Introduction

We analyzed the results of a triple collocation experiment performed at the OCA (Observatoire de la Côte d'Azur) at Grasse (France) between September and November 2001. This experiment involved the 3 OCA laser systems: the classical fixed satellite laser ranging station (SLR) station, the Lunar Laser Ranging station (LLR), and the French transportable Laser Raging Station (FTLRS). The analysis of the LAGEOS common normal points indicated a systematical range bias of (13 ± 1) mm between the SLR and the LLR (Nicolas et al., 2002). From laboratory experiments, we explained 9 mm linked to the center-edge effect of the APD (Avalanche Photo Diode) and to the velocity aberration for the LLR station. The aim of this study was thus to explain the residual 4 mm. We evaluated the LAGEOS satellite response differences between these two instruments. For this purpose we used geometrical considerations on the satellite and station instrumental differences.

From the satellite geometrical characteristics, we computed the contribution of each retroreflector corner cube row and the satellite response for a laser beam corresponding to each station. Then, we compared these responses to the raw data of each laser system. Finally, we deduced the corresponding range bias and the center of mass correction to apply to each laser station.

Herein, we first summarize the LAGEOS –1 and –2 satellites characteristics and the OCA SLR and LLR station instrumental differences. Then, we present the method used for the satellite response computation and the comparison of this response with the real response observed by the two stations. Finally, we present the results in terms of bias difference between the two systems and of center of mass correction.

2. LAGEOS satellites

The LAser GEOdynamics Satellite –1 (LAGEOS –1, 1976) and LAGEOS –2 (1992) satellites (see Figure 1) with an altitude of about 6000 km are reference targets for accurate laser station positioning, providing a permanent reference point with a very stable orbit. Both satellites are similar (sphere of 60 cm diameter and about 400 kg weight) and have a high mass-to-area ratio of about 1450 kg/m_. These very dense satellites are also the primary targets used in quality controlling data from the international satellite laser ranging network. Their inclinations are of 110° and 53°, respectively (see Figure 2).

Figure 1: LAGEOS satellite

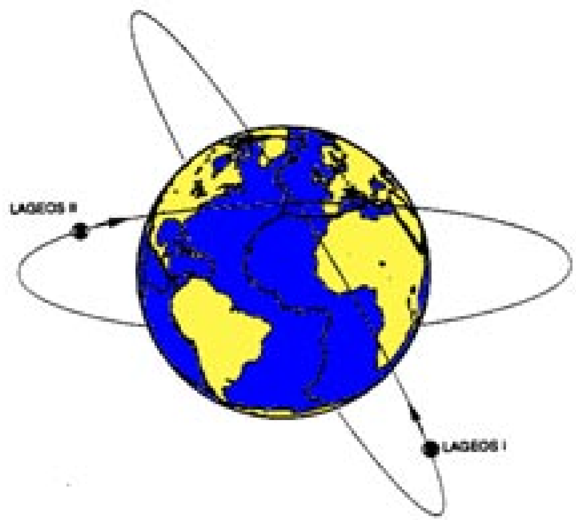

Figure 2: LAGEOS –1 and –2 orbits

The LAGEOS satellites are covered with 426 Cube Corner Reflectors (CCRs), 422 being made of fused silica glass. The other four CCRs are made of germanium to obtain measurements in the infrared for experimental studies of reflectivity and satellite orientation. The 4 germanium CCRs are differently located on LAGEOS –1 and LAGEOS –2. But it does not matter in our study since we treated all the CCRs as made of silica. The satellites are constituted by two hemispheres covered with 10 rows of CCRs (see Figure 3). Table 1 indicates the number of CCRs and the disposition of each row on the LAGEOS –1 satellite (Avizonis, 1997).

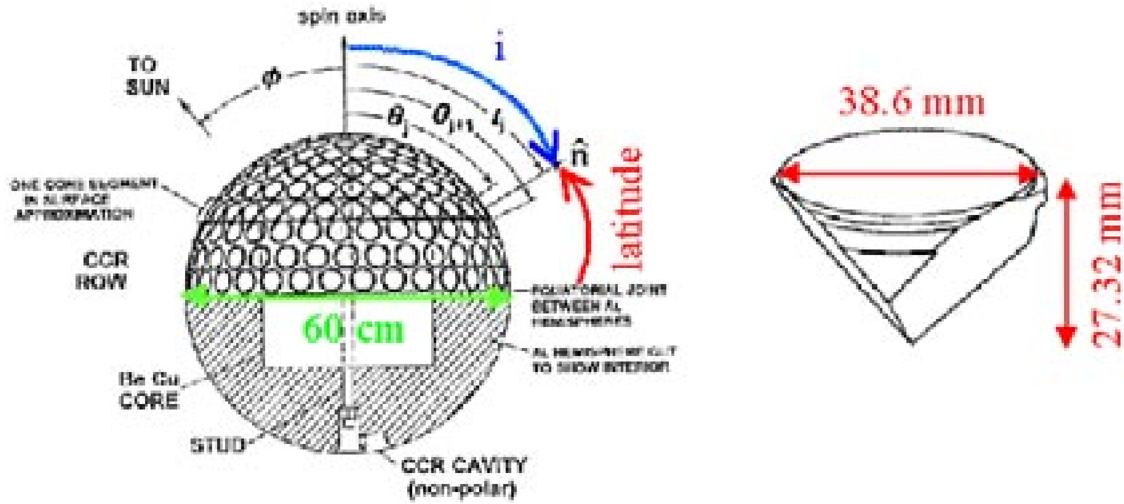

Figure 3: Repartition and dimensions of the CCRs on the LAGEOS satellite (Slabinski, 1997).

Table 1: Number of CCRs on each row on the LAGEOS satellite (Avizonis, 1997). The star (*) indicates the Germanium CCRs on LAGEOS –1.

row number	CCR number	Latitude (°)
1	1 *	90.00
2	6	79.88
3	12	70.15
4	18	60.42
5	23	50.69
6	27	40.96
7	31	31.23
8	31	22.98
9	32	13.25
10	32	4.86
11	32	- 4.87
12	32	-13.25
13	31 *	-22.98
14	31	-31.23
15	27	-40.96
16	23	-50.69
17	18	-60.42
18	12	-70.15
19	6	-79.88
20	1	-90.00

3. Grasse SLR and LLR station characteristic differences

The technical feature differences between the OCA SLR and LLR stations are summarized in Table 2. The main differences are the laser pulse width, the return detector, and the detection level. These aspects are taken into account in the satellite response computation.

Table 2: Grasse Satellite Laser Ranging (SLR) and Lunar Laser Ranging (LLR) main features.

	SLR	**LLR**
telescope diameter	1.00 m	1.54 m
laser	Nd:YAG 532 nm 40 ps 10 Hz divergent	Nd:YAG 532 nm 20 ps 10 Hz parallel beam
calibration	semi-internal post-pass	internal real time
return photodetector	C-SPAD	APD
return level	multi-photon	single photon

4. Method of computation

For the satellite response computation, we used the following method. Firstly, we computed the contribution of each CCR row in the reflected signal for a given incident angle and a given pulse width. Then, we computed the corresponding delay for each CCR row and a satellite response histogram (summation of each CCR row contribution). Afterwards, we adjusted this response amplitude to the real satellite response (raw data). Finally, we deduced the corresponding bias for each station, the value of the range bias difference between LLR and SLR systems, and the satellite center of mass correction for each system.

At this point, it is important to do some remarks concerning this computation. First of all, we performed this computation for the single photon electron detection case and we performed the comparison with LAGEOS –2 raw data. We considered the 426 CCRs as made of fused silica, even if 4 are made of germanium. We also made the hypothesis of an homogeneous repartition of the CCRs on the satellite, even if they don’t have exactly an homogeneous distribution. Moreover, we ignored the CCRs recess of 1 mm behind the satellite surface and treated the CCRs as coplanar with the satellite surface. We also ignored the satellite spin, considering that during a pass, the satellite completes several rotations. In addition, we neglected the differences of the optical path inside the CCRs depending on the incident angle. But, all these points may only induce a small difference of the satellite response computation.

4.1 Contribution of each row of CCRs

In a first step, we computed the contribution of each row of CCRs to the satellite response. The contribution P of a single row is defined by: $P = N_{CCR} \times R_{CCR} \times \cos i$, where N_{CCR} represents the number of CCRs of the considered row, R_{CCR} corresponds to the CCR reflectance, and i is the incident angle of the laser beam on the CCR. We defined the first row as the one where the laser beam meets the satellite surface. We considered the CCR of the first row as an arbitrary reference unit. Thanks to our hypothesis of homogeneity, we considered that the distribution of the CCRs around this first CCR is similar to the distribution around a polar CCR given in Table 1. The CCR reflectance curve used is given by Figure 4 (Avizonis, 1997). The results are summarized in Table 3. Due to the fast decreasing of the reflectance when i is increasing, the contributions of the rows 8 and 9 are negligible and that the ones of the other rows up to the 9^{th} are not visible or cannot be detected.

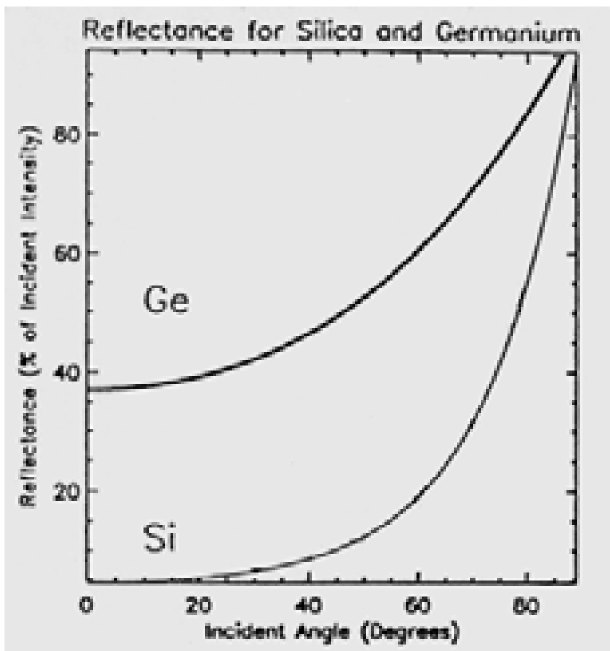

Figure 4: LAGEOS CCR reflectance curve (Avizonis, 1997).

Table 3: Contribution P of each row of CCRs of LAGEOS satellite.

Row	N_{CCR}	R_{CCR}	cos i	P
1	1	1	1	1
2	6	0.5	0.984	2.953
3	12	0.3	0.940	3.386
4	18	0.2	0.870	3.131
5	23	0.1	0.770	1.780
6	27	0.05	0.510	0.885
7	31	0.02	0.656	0.406
8	31	0.01	0.390	0.121

4.2 Delay of each row of CCRs

In a second step, we computed the delay *d* between each row of CCRs using the following relation between the geometrical parameters of the satellite, namely its radius *R* and the laser beam incident angle *i*: $d = R(1 - \cos i)$. The angle *i* is defined as showed on Figure 5. Table 4 gives the delays computed in millimeters for each row of CCRs.

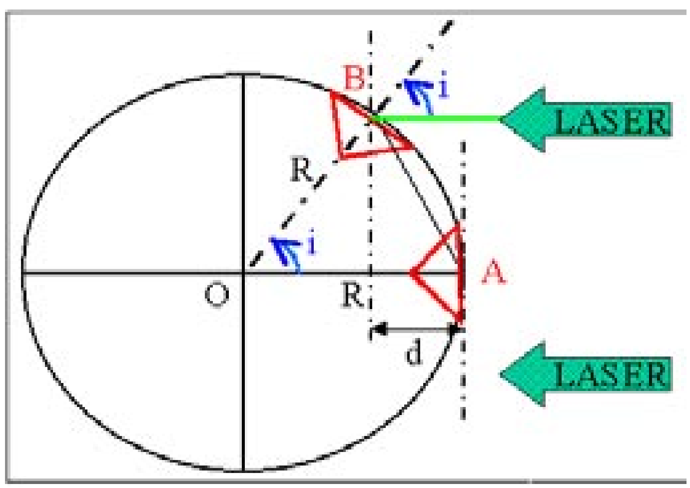

Figure 5: Geometrical parameters used for the computation.

Table 4: Delay of the contribution of each row of CCRs to the LAGEOS satellite response.

Row	**d (mm)**
1	0
2	4.7
3	17.8
4	39.1
5	67.9
6	103.3
7	144.5
8	182.9

Nevertheless, for a correct computation we had to take into account the position of the mean laser beam impact on the satellite surface. For this, we considered two extreme cases (see Figure 6). In the first one, the mean impact point corresponds to a CCR face in front of the satellite. In the second case, the mean impact point meets the satellite surface among 3 distinct CCRs. All the previous computations were performed in the first case. Real cases stand between these two extreme cases. We computed the range delay between these two cases. At the satellite equator, there are 32 CCRs, that is to say one CCR every 11.25°. Between a mean impact point perpendicular to a CCR surface and a mean impact among three distinct CCRs, the angle changes by about 8.5°. Then, the corresponding difference on the range measurement is of about 3.3 mm, that is to say 22 ps. Because of the satellite rotation, all the configurations are present, but they are always comprised between these two extreme cases. Thus, in order to take this into account, we added a statistical widening of 22 ps of the CCR row response.

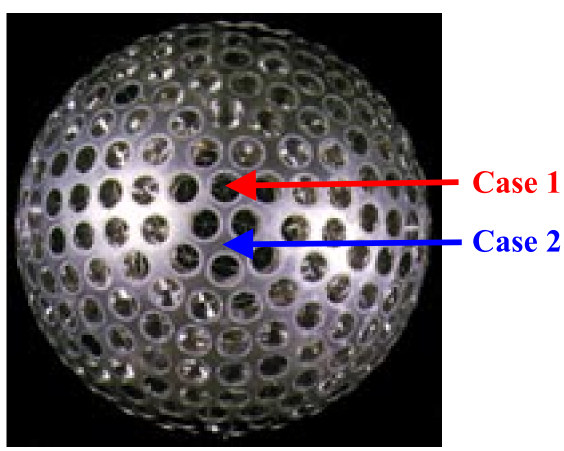

Figure 6: Difference of the mean impact point position on the LAGEOS satellite surface between the two extreme cases. In the case 1, the mean impact point corresponds to a CCR face. In the case 2, the impact point meets the satellite surface among 3 distinct CCRs.

4.3 Satellite response

We computed the satellite response as the convolution of gaussian curves with:
- a shift given by the delay of each row of CCRs,
- the widening of 22 ps computed previously due to the satellite spin, and
- a width corresponding to each station response (depending on the laser, on the photo-detector, on the atmosphere...).

For these widths, we used the following realistic values from laboratory measurements:
- 63 ps for the LLR (50 ps from the laser station),
- 48 ps for the SLR (40 ps from the laser station).

We computed the satellite response with a gaussian curve, even if we know that the photodiode response is not exactly a gaussian one (especially for the C-SPAD and thus for the SLR station). We also considered a uniform laser energy distribution on the satellite.

5. Model and raw data comparison

5.1 Results with the LLR data

The next step of the analysis was the comparison between the satellite response computed with the method described above and the real raw data of each system. We computed the satellite response as the empirically weighted sum of each CCR row response. Figure 7 illustrates the comparison between the modeled satellite response and a LAGEOS –2 LLR pass of the 16th October 2002, for which there are 5,667 measurements. This comparison indicates that the contribution of the rows from the number 4 are over-estimated. It also shows the very low contribution of the rows greater than the 5^{th} because of their delays from the first row. This over-estimation is linked to the CCR limit incident angle, which amounts to 35°.

So, we adjusted empirical attenuation coefficients from the raw data comparison. These coefficients are indicated in Table 5. These values indicate that the main contribution of the satellite response is given by the three first rows of CCRs. The lower contribution of the other rows can be explained by the greatest probability of detection of the photons coming back from the nearest rows of CCRs. These coefficients characterize the satellite response for a given laser system. There are nearly the same for all the passes considered in this study, the differences are due to small energy level variations between the different passes. Figure 8 shows the model and data comparison for the same pass.

Then, we can see that there is a fairly good agreement between the real data and our computation of the satellite response.

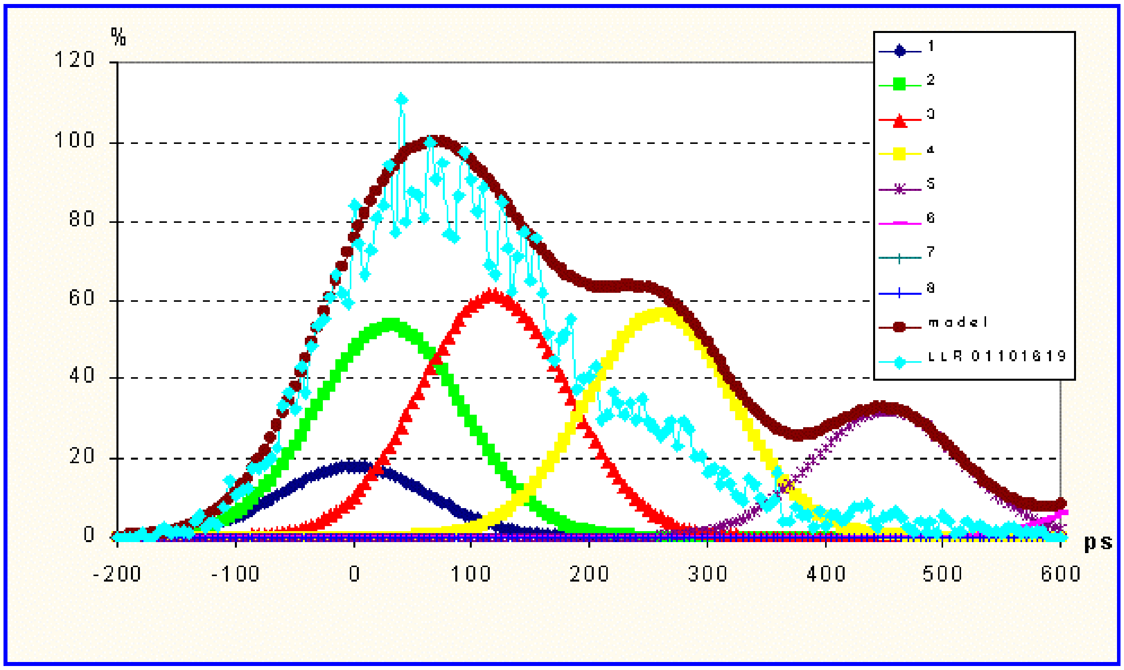

Figure 7: LAGEOS –2 pass of the 16th October 2001. The contribution of each row of CCRs up to the 8th and the final model obtained with the convolution of each row contribution (in brown) are represented. The cyan curve corresponds to the real raw data observed by the OCA LLR station.

Table 5: Empirical attenuation factors of the model for the contributions of the different LAGEOS rows of CCRs for the Grasse LLR station.

Row	**Coef.**
1	1
2	1
3	1
4	0.4
5	0.14

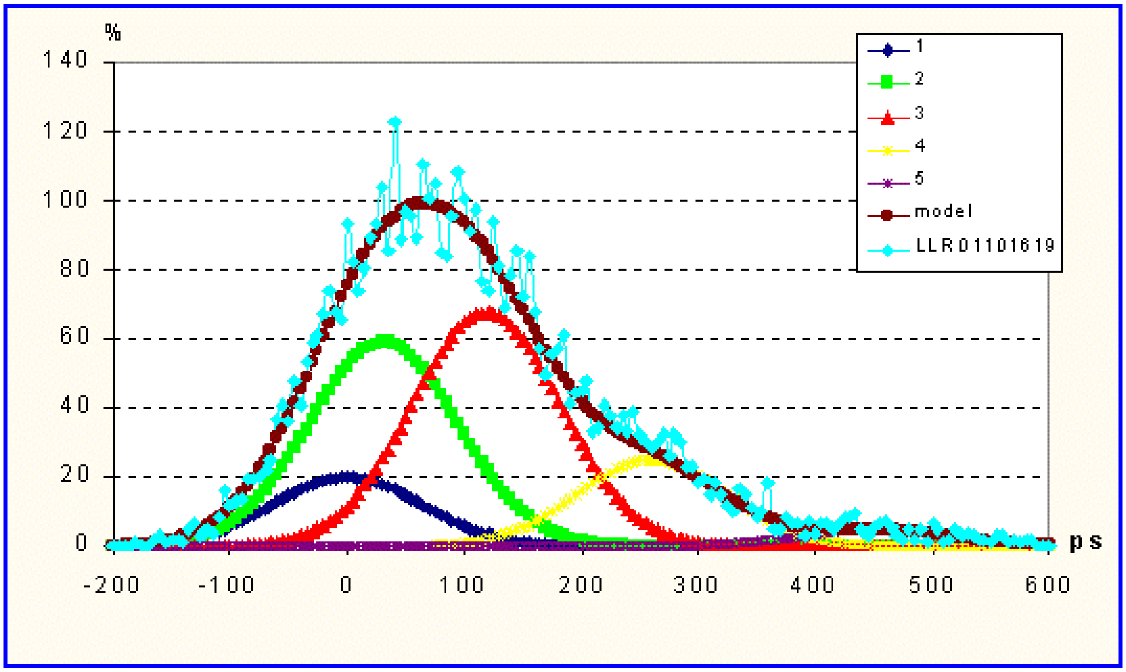

Figure 8: Comparison between the LAGEOS –2 LLR raw data (pass of the 16th October 2001) and the satellite response model with the attenuation factors. The contribution of each row up to the 5th are also indicated.

5.2 Comparison with SLR measurements

The comparison between the modeled satellite response and the SLR raw data showed also a difference due to non adapted attenuation factors. Indeed, these coefficients differ from the ones computed with the LLR data since these two instruments have not exactly the same technical features. Figure 9 gives the example of a LAGEOS –2 pass of the 17th October 2001 observed by the OCA SLR station (9,591 observations) and the comparison between these raw data and the model. Table 7 indicates the empirical attenuation coefficients adjusted for the SLR case. The differences between the LLR and the SLR cases are mainly linked to the non gaussian curve for the C-SPAD response instead of the APD for the LLR station and to the multi photo-electron detection level instead of a single photo-electron detection level for the LLR.

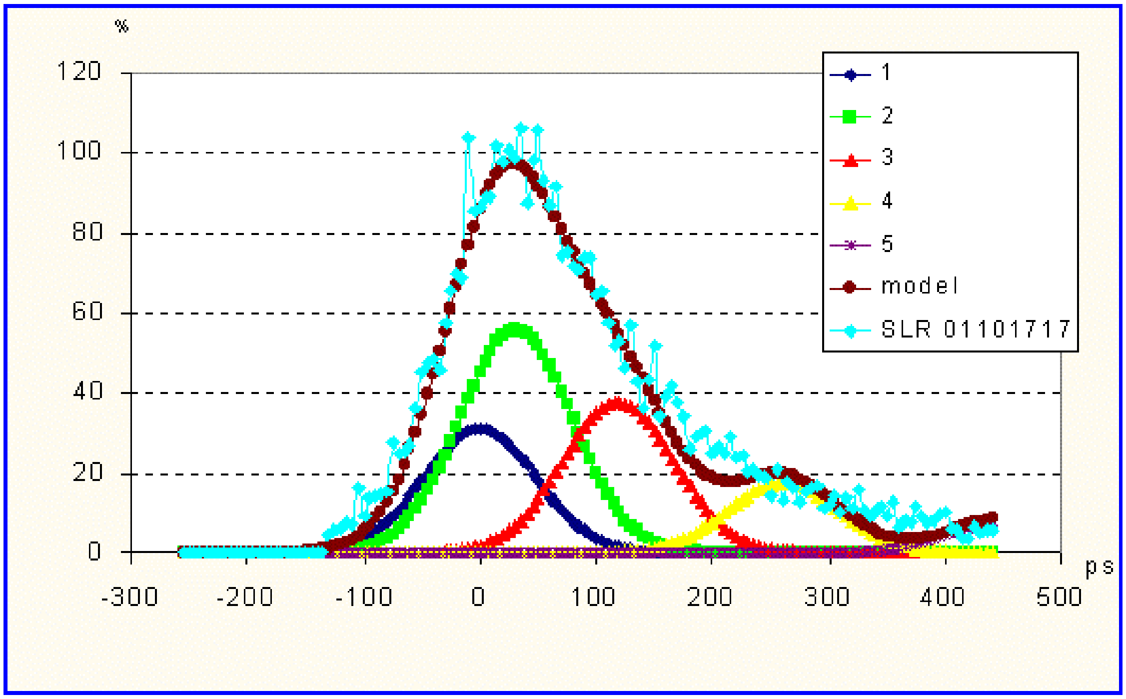

Figure 9: LAGEOS –2 pass (17th October 2001). Comparison between the OCA SLR raw data (cyan) and the computed model (brown). The contribution of each row up to the 5th to the satellite response are also indicated.

Table 7: Empirical attenuation factor of the model for the different CCRs row contribution for the SLR station.

Row	**Coef.**
1	1
2	0.61
3	0.36
4	0.18
5	0.14

6. Bias computation and center of mass correction

From this satellite response model computation, we estimated a **range bias** *B* from a unique CCR at the LAGEOS satellite surface. For this, we used the following equation: $B = \frac{\sum_i d_i \times P_i \times coeff_i}{\sum_i P_i \times coeff_i}$.

The resulting mean biases computed on the different passes are of (14.8 ± 2) mm for the LLR station and of (11.8 ± 2) mm for the SLR station. But we have to add the bias of 9 mm for the LLR station due to the center-edge effect of the photodiode and to the velocity aberration on LAGEOS. In conclusion, we find a range bias difference between the LLR and the SLR stations of 12 mm. At this point, we should remind that the results of the collocation experiment gave a range bias difference of (13 ± 1) mm between these two systems (Nicolas et al., 2002). So, with this quite simple model, we explain at the 1 mm level the systematical error between these two stations with realistic empirical evaluations.

Finally, from these computations, we also estimated the **center of mass correction** of the LAGEOS satellite. For this computation, we defined the reference point of a virtual unique CCR with: $r_{sat} - l_{CCR} \times n_{CCR}$=259 mm, where r_{sat} is the satellite radius, l_{CCR} is the CCR depth of 27.32 mm (see Figure 3), and n_{CCR} is the CCR refraction index (1.5 for the fused silica). The center of mass correction is computed as the difference between the reference distance and the computed station range biases. Then, we found a center of mass correction of 244 mm for the LLR station and of 247 mm for the SLR station (see Figure 10). Whereas the standard center of mass correction value amounts to 251 mm. Thus, it indicates that the center of mass standard value is not consistent with the value found from the OCA laser station data analysis and that this correction depends on the considered laser system.

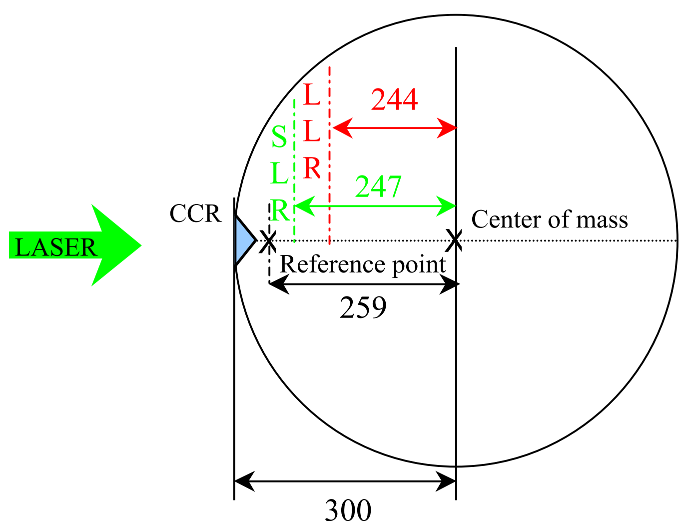

Figure 10: Center of mass corrections in millimeters for the different Grasse SLR and LLR stations for the LAGEOS satellites.

7. Conclusion

In conclusion of this study, we can say that we can explain the difference observed between the OCA SLR and LLR stations at the level of 1 mm by geometrical considerations. We also made obvious that the satellite signature and the center of mass correction depend on the laser station characteristics. This study also shows the great importance of the raw data analysis since all these computations could not have been performed only with the normal points.

Furthermore, a remark comes out from this study to reach the millimeter accuracy with the satellite laser ranging technique: we suggest the ILRS to compute tables of center of mass corrections for each satellite and each station, as it was nearly done for TOPEX/Poseidon (T/P), and to take care of the update of these tables. For instance, nowadays an update is needed for the T/P center of mass correction since it is not suited for some European stations (see Nicolas et al. paper in the session "station performance evaluation" of this workshop). From now on, it seems possible to reach the millimeter accuracy with the SLR technique, but it implies to take into account many aspects until now often considered as more or less negligible. Indeed, the actual capabilities of the ILRS network underscore new critical points such as this satellite signature dependence on the laser system technical features.

8. Acknowledgements

We are grateful to the OCA SLR and LLR laser teams, and especially for their effort to perform common LAGEOS observations. This study is supported by CNES, INSU, CNRS, and the French Ministry of Research.

9. References

Avizonis P.V., *Remote sensing of the LAGEOS-1 spin axis and image processing for advanced optical systems*, Ph.D. Thesis, University of Maryland at College Park, 1997.

Nicolas J., P. Bonnefond, O. Laurain, Ph. Berio, P. Exertier, and F. Barlier, *Triple laser ranging collocation experiment at the Grasse observatory, France*, Phys. Chem. Earth, in press, 2002.

Slabinski V.J., *A numerical solution for LAGEOS thermal thrust: the rapid spin case*, Celest. Mech., **66**, **131**, 1997.